DR. LORENZO TAVELLI (Orcid ID : 0000-0003-4864-3964)

DR. SHAYAN BAROOTCHI (Orcid ID : 0000-0002-5347-6577)

DR. HSUN-LIANG CHAN (Orcid ID : 0000-0001-5952-0447)

PROF. WILLIAM V. GIANNOBILE (Orcid ID : 0000-0002-7102-9746)

PROF. HOM-LAY WANG (Orcid ID : 0000-0003-4238-1799)

Article type : Clinical Innovation Report

Ultrasonographic Tissue Perfusion Analysis at Implant and Palatal Donor Sites Following Soft Tissue Augmentation: A Clinical Pilot Study

Lorenzo Tavelli[1], DDS, MS, Shayan Barootchi[1], DMD, Jad Majzoub[1], BDS, Hsun-Liang Chan[1], DDS, MS, William V. Giannobile[1,2], DDS, MS, DMSc, Hom-Lay Wang[1], DDS, MSD, PhD, Oliver D. Kripfgans[2,3], PhD

[1] Department of Periodontics & Oral Medicine, University of Michigan School of Dentistry, Ann Arbor, MI, USA

[2] Biointerfaces Institute and Department of Biomedical Engineering, College of Engineering, Ann Arbor, MI, USA

[3] Department of Radiology, University of Michigan Medical School, Ann Arbor, MI, USA

Corresponding author

Hsun-Liang Chan, DDS, MS

Department of Periodontics and Oral Medicine

University of Michigan School of Dentistry

1011 North University Avenue

Ann Arbor, Michigan 48109-1078, USA.

E-mail address: hlchan@umich.edu

Word count (without references): 2995

Tables and figures: 4 tables and 7 figures

Supplementary files: 2 supplementary videos

Running title: Tissue perfusion analysis at implant sites

One sentence summary: Application of power Doppler Ultrasonography for evaluating blood flow at implant and palatal donor sites following soft tissue augmentation with the connective tissue graft.

Acknowledgment and conflict of interest: The study was supported by grants from the National Institute of Dental and Craniofacial Research (NIDCR) R21 grant (1R21DE027765 – 01A1 and 1R21DE029005-01A1), National Center for Advancing Translational Sciences of the National Institutes of Health Award (UL1TR000433), Delta Dental Foundation (AWD010089 and AWD004687), American Academy of Periodontology Sunstar Innovation Award (AWD007224), and University of Michigan Department of Periodontics and Oral Medicine Clinical Research Grant (N026036). The authors do not have any financial interests, either directly or indirectly, in the products or information enclosed in the paper.

Author contributions: L.T., S.B., H.L.C., W.V.G, H.L.W. and O.D.K. contributed to the conception and design of the work. L.T., H.L.C. and J.M. contributed to the collection of the data, O.D.K. computed the data and S.B. analyzed the data. L.T., S.B., H.L.C and O.D.K. designed the schematic illustrations. L.T., S.B., and O.D.K led the writing; H.L.C., W.V.G, J.M. and H.L.W. critically reviewed and contributed to the writing of the manuscript.

ABSTRACT

Aim: To describe the application of power Doppler Ultrasonography (US) for evaluating blood flow at implant and palatal donor sites following soft tissue augmentation with the connective tissue graft (CTG).

Materials and Methods: Five patients exhibiting a per-implant soft tissue dehiscence received treatment with a coronally advanced flap and corresponding CTG. Power Doppler US was used for assessing blood volume at baseline, 1 week, 1 month, 6 months and 12 months post-surgery for assessing blood flow dynamics at the implant and palatal donor sites. The speed-weighted and power-weighted color pixel density (CPPD) were computed from color velocity (CV) and color power (CP), respectively.

Results: A mean increase in CV of 199.25% was observed at the midfacial region of the implant sites after 1 week compared to baseline. CV and CP were increased in all sites at 1 week and 1 month. At 6 and 12 months, the mean CV appeared lower than baseline at the implant sites. CCPD was increased at the palatal donor sites and at the great palatine foramen areas at the 1-week and 1-month post-operative evaluations.

Conclusions: Power Doppler US is a non-invasive and valuable tool for estimating tissue perfusion and CPPD variation during different phases of intraoral soft tissue graft healing

Key words: Blood flow circulation, Blood supply, Blood flow velocity, Dental implant, Ultrasonography, Soft tissue augmentation, Connective tissue graft

Clinical relevance

Scientific rationale for the study: Non-ionizing, real-time ultrasonography (US) has shown to be a valuable tool for evaluating soft and hard tissues. Another advantage of US is the evaluation of blood flow and tissue perfusion with power Doppler ultrasonography. This technology is routinely used in medicine, however, its applicability in the oral cavity has not yet been explored to the best of our knowledge. This study describes a method for using US for assessing blood flow variation in terms of color and power pixel density (CPPD) at the implant and palatal donor sites following augmentation with connective tissue grafting procedures.

Principal findings: US power Doppler captured and estimate tissue perfusion at different time points at implant and palatal sites, with the 1-week and 1-month follow-up showing the greatest increase in CPPD. Blood volume at 6 and 12 months was reduced compared to baseline at the implant sites.

Practical implications: The use of US power Doppler is a non-invasive and suitable tool for estimating tissue perfusion and CPPD variation during different phases of wound healing. This method may become useful in the future in identifying conditions with abnormal blood flow or subclinical inflammation.

1. Introduction

Over the past decade, technological advancements have had major impact in dentistry by changing the way that oral health care is delivered. Non-ionizing, cross-sectional and real-time ultrasonography (US) is a promising imaging modality that serves as a valuable tool for evaluation of vital anatomical structures, and soft and hard tissue dimensions (Barootchi et al., 2020a, Chan et al., 2017a, Bhaskar et al., 2018, Chan and Kripfgans, 2020b). Recently, studies have validated the accuracy of US compared to histology or cone-beam computed tomography (Barootchi et al., 2020a, Chan et al., 2017a, Chan et al., 2018, Tattan et al., 2019). Another unique advantage of US is the functional soft tissue evaluation, i.e., blood flow and tissue perfusion. As different pathological states are characterized by altered vascularity in perfusion (Levy et al., 2008), perfusion estimation has been explored in medicine with numerous technologies. Among them, power Doppler US, a technique introduced to overcome the limitations of color Doppler US (Rubin et al., 1994). This new scanning-angle independent approach integrates the color flow power spectrum which extends the dynamic range and increases the machine's sensitivity to blood flow versus the traditional mean frequency estimator that is prone to noise for reduced flow (Rubin et al., 1994, Bude et al., 1994, Newman et al., 1994). In addition, power Doppler ultrasound has advantages for blood flow (color and power) quantification because of its ability to depict low-velocity signals and multidirectional flow and its lack of aliasing (Rubin et al., 1994, Welsh et al., 2019). To compensate for possible signal attenuation due to depth and tissue inhomogeneity, a method termed fractional moving blood volume (FMBV) has been established (Rubin et al., 1995, Welsh, 2004). This technique is based on the cumulative power distribution function to define a stable intravascular point, providing an absolute value for vascularity for inter- and intra-case comparisons (Rubin et al., 1997, Welsh et al., 2019). FMBV evaluation requires an offline image analysis technique applied to raw exported three-dimensional (3D) power Doppler US (Stevenson et al., 2015, Welsh et al., 2019). This method has been used to assess blood flow and perfusion of the kidney (Welsh et al., 2019), optic nerve (Vosborg et al., 2020), placenta (Lai et al., 2010) and fetal organs (Hernandez-Andrade et al., 2007, Hernandez-Andrade et al., 2004b), among others.

It is possible that this non-invasive and real-time technology becomes an accurate and cost-effective tool for evaluating periodontal tissue perfusion. Detecting subclinical inflammation before the occurrence of periodontal or peri-implant bone loss could be one of the potential benefits of US (Chan and Kripfgans, 2020b). In addition, power Doppler US could also explore blood flow changes following soft tissue grafting, which might relate to the course of wound healing and the final clinical outcomes. In particular, blood volume analysis at grafted implant sites could provide further insight about the effect of phenotype modification on peri-implant health, as inflammation accompanies changes in tissue perfusion. The current clinical method of staging inflammation by "bleeding on probing" is subjective, and relative to implants still controversial (Hashim et al., 2018, Renvert et al., 2018, Barootchi et al., 2020b). Another possible application of power Doppler US includes the

evaluation of palatal donor site perfusion during different phases of wound healing. Having the advantages of being point-of-care, cost-efficient, and non-ionizing, US can become a convenient and an objective tool for research and for routine clinical practice for estimating tissue perfusion and possible would healing outcomes in research and clinical care arenas. Therefore, the aim of the present manuscript was to demonstrate the application of novel power Doppler US for assessing the alterations in blood flow and tissue perfusion at implant and palatal sites during the healing process after soft tissue augmentation with a connective tissue graft (CTG).

2. Clinical innovation report

2.1 Study registration, design and participants

Five periodontally and systemically healthy patients with esthetic concerns regarding a dental implant diagnosed with peri-implant soft tissue dehiscence/deficiency (PSTD) (Zucchelli et al., 2019) requiring a treatment were selected from the Department of Periodontics and Oral Medicine, School of Dentistry, University of Michigan, Ann Arbor, USA. Further details of the inclusion and exclusion criteria are presented in the Appendix. The study was in accordance with the Institutional Review Board of the University of Michigan Medical School (HUM00140205) and was in accordance with the Declaration of Helsinki of 1975, revised in Tokyo in 2004.

2.2 Surgical procedures

All surgical procedures were performed at the same clinic (Department of Periodontics and Oral Medicine, University of Michigan), by a single operator (L.T.). PSTDs were treated with an envelope split-full-split thickness coronally advanced flap (eCAF) + CTG as previously described by Zucchelli et al. (Zucchelli et al., 2013, Zucchelli et al., 2019). The CTGs were obtained as an epithelialized gingival graft from the premolar areas on the palatal regions and were extraorally de-epithelialized. The palatal wounds were covered with a collagen dressing (Collatape, Zimmer Biomet, USA) and secured with cross sutures (5/0 Vicryl, Ethicon, Johnson & Johnson, USA). A few drops of cyanoacrylate tissue glue (PeriAcryl 90 HV, Glustitch, Delta, Canada) were applied over the palatal wounds on top of the collagen dressing (Tavelli et al., 2019b, Tavelli et al., 2018). Presurgical procedures, surgical approaches and post-operative protocols are described in detail in the Appendix.

2.3 Ultrasound images acquisition

The ultrasound equipment setup and the scanning procedures were performed by two experienced operators with expertise in the field of ultrasonography (H.C. and O.K.) (Chan et al., 2017a, Chan et al., 2017b, Barootchi et al., 2020a, Chan and Kripfgans, 2020b, Tattan et al., 2019). The scans were taken at baseline (prior to the initiation of the surgical procedure), and at 1-week, 1-month, 6-month and 12-month follow-up appointments at both the implant recipient, and palatal donor sites. A commercially available ultrasound imaging device (ZS3, Mindray, Mountain View, CA) as described

in previous reports (Chan et al., 2017b, Barootchi et al., 2020a, Chan and Kripfgans, 2020b) coupled with a 24 MHz (64 μm axial image resolution) and miniature-sized (approximately 30 mm long, x 18 mm wide x 12 mm thick) probe prototype (L25-8) was used to generate ultrasound images (Figure 1). As ultrasound is a real-time imaging modality, two types of images ("still" and "cine loops") were recorded and stored. A "still image" presents a single 2D image frame, while "cine loops" are videos that are generated as result of the collection of consecutive still images. Both image types were saved in the Digital Imaging and Communications in Medicine (DICOM) format. US "B-mode" generates 2D grey-scale images in which brightness is determined by the envelope of the returned echo signal. The strength of the echo signal depends on the mechanical properties of the involved soft and hard tissues (Figures 2 and 3).

US is either scattered or reflected. Structures much smaller than the acoustic wavelength (λ=64 μm) scatter the ultrasonic waves in all directions, whereas large structures reflect the ultrasonic wave obeying Snells' Law. (Chan and Kripfgans, 2020a).

"Color flow" is an imaging mode in which the B-mode display is overlaid with additional color pixels that represent detected blood flow. In this case B-mode provides an anatomical reference for the physical location of the detected blood flow (Chan and Kripfgans, 2020b). "Color flow", also known as "color Doppler", detects phase-changes in the received US signal. Red blood cells scatter US. Flowing red blood cells produce a scattered signal that changes in phase as long as the direction of the motion is non-perpendicular to the US beam. The largest phase shift is seen when blood flows in the direction of the US beam and no phase-shift is observed when the flow is perpendicular to the beam. In particular, color flow computes the mean phase change, i.e. the mean velocity, that is derived from the detected US signal. Therefore, color flow mode utilizes color Doppler signals, displaying blood-flow direction and relative velocity, with shades of red and blue colors assigned to image pixels based on the flow direction and velocity. In particular, the color red indicates blood flow towards the transducer, while blue color denotes blood flow in the opposite direction (Figure 4). Lack of color pixels can be interpreted as either no blood flow or blood flow perpendicular to the US beam. Live scanning allows the operator to position the US probe in a way that is most representative of the given vascular anatomy.

The displayed color velocity (CV) is the projection of the actual velocity onto the US beam, which mathematically equals the multiplication of the true velocity by the cosine of the angle to the US beam. CV data are filtered using a "wall filter" to eliminate tissue motion of the adjacent vascular walls (Chan and Kripfgans, 2020b). CV visualizes the speed at which blood flows within the lumens in the field of view. For higher tissue perfusion higher velocities might be observed. "Color power" (CP) is an imaging mode that is also based on detecting phase-change of the received US signal. However, instead of displaying the mean velocity, it displays the integrated power of the received US signal after the wall filter has been applied. This power is displayed in a single-hue red color (Figure 4). Since the power is derived after the wall-filter has been applied, CP visualizes the *amount* of blood

flowing within the lumens in the field of view and it is particularly useful for small vessels and those with low-velocity flow. For higher tissue perfusion, more blood vessels might be active, and the vasculature might also show vasodilation, thus more blood might be flowing.

2.4 Areas of interest

The areas of interest at the implant site were: i) midfacial, ii) mesial (at the line angle between the crown and the mesial papilla), iii) distal (at the line angle between the crown and the distal papilla) and iv) transverse scan at 3 mm from the mucosal margin level (Chan and Kripfgans, 2020b). For the midfacial, mesial and distal scans, the US probe was oriented parallel to the long axis of the implant and perpendicular to the occlusal plane, while for the transverse scan the probe was oriented parallel to the occlusal plane. The areas of interest at the palatal donor site were: 3-, 5-, and 8-mm reference points apical to the gingival margin of the first and second premolars, and the greater palatine foramen (GPF) area, which was identified by palpation at the junction between the horizontal plate of the maxilla and alveolar ridge at the 3rd molar location (Fu et al., 2011, Tavelli et al., 2019a). For each area of interest at the implant and palatal site, B-mode, CV and CP scans were performed and saved as still images (for the B-mode) and cine loop videos (for CV and CP modes) at the baseline, 1 week, 1 month, 6-months and 12-months.

2.5 Ultrasound image analysis and blood volume calculation

As a preliminary analysis, ultrasonography measurements were taken of the mucosal recession depth (MRec), mucosal thickness (MT) and palatal thickness (PT) on the B-mode images using a commercially available software package (Horos™, version 3.3.6, Horos Project), as previously described (Chan and Kripfgans, 2020b). All the measurements were carried out by a single calibrated and experienced examiner (J.M.) who is an active member of the dental ultrasonography laboratory and has been conducting extensive US periodontal/peri-implant measurements for the past 2 years. Additional details are also listed in the Supplementary Appendix.

The speed-weighted color pixel density and power-weighted color pixel density (CPPD) was computed from CV and CP, respectively. For such, a ROI on the soft tissue of interested was identified. For the implant site, the ROI was defined as the area between the soft tissue margin and extending 7 mm apically, while for the palatal scans, the entire the soft tissue above the palatal bone was used as ROI (Figure 5). The color pixel information from within the ROI were extracted using the displayed color- and power-bar to decode the underlying velocities and power (Chan and Kripfgans, 2020b).

It should be noted that color velocity imaging was performed using a constant velocity scale (±2.3 cm/s) to maintain the same wall filter for all cases. This opens the possibility for aliasing in the color velocity image, i.e. velocities larger than +2.3 cm/s or smaller than -2.3 cm/s, will lead to the positive/negative velocity scale, respectively. Affects to the speed-weighted color pixel density is,

however, minimized by using the absolute measured velocities, i.e. negative velocities are negated to obtain positive velocities. The CV and CP gain was also kept the constant throughout the study in order to warrant sensitivity (velocity and power) and to ease the comparison of velocity power values from individual scans and patients.

Speed-weighted (CV_w) and power-weighted (CP_w) color pixel densities were computed by a calibrated examiner with expertise in ultrasound imaging and image/signal processing (O.K.) using custom scripts for Matlab (The Mathworks, Natick, MA) (Supplementary Video 1). All data were processed using the same scripts to improve scientific rigor and eliminate bias.

CV_m and CP_m were obtained as an average of CV/CP_w across at least 5 the cardiac cycles (6 second cine clips at minimum 20 Hz frame rate for cardiac averaging). The variation in percentages compared to baseline was computed and descriptive statistics were used to present the gathered data as means ± standard deviations (SD).

3. Results

3.1 Experimental population and baseline characteristics

Five female patients (mean age 52.2 ± 11.1 years), each with a single PSTD were consecutively treated with a eCAF + CTG. All PSTDs extended until the abutment component alone, without exposure of the implant fixtures to the oral cavity. Baseline characteristics and blood volume before the surgery (baseline) are depicted in Tables 1 and 2 and in the Appendix.

3.2 Imaging interpretation

Figure 2 showed representative US images taken in the abovementioned 4 locations. In the mid-facial slice, the implant-supported crown surface appeared as a hyperechoic (bright) band with relatively uniform (apparent) thickness along its length. The abutment surface, also a hyperechoic structure, followed the crown in an apical position. The implant fixture surface was also visible as a uniform hyperechoic band, with possible thread appearance if exposed. The bone surface was identifiable as a bright curved line. The peri-implant mucosa appeared as a hypoechoic (dark) band surrounding the abutment, implant fixture and bone. The mesial and distal scans showed the interproximal soft tissue between the bone crest and the papilla tip. The transverse scan showed the implant abutment in the middle of the image as a hyperechoic semicircular structure, the facial alveolar bone surface in front of the two adjacent teeth, and the investing hypoechoic overlying soft tissues. The palatal scans showed hypoechoic palatal mucosa between the two hyperechoic lines running relatively parallel between them. The superior hyperechoic line is the soft tissue surface, while the inferior represents is the palatal bone. A similar imaging was observed at the GPF area, except for the soft tissue shaping as a funnel at the foramen site through which the neurovascular bundles leave the oral cavity for the pterygopalatine fossa. The palatal bone showed as a discontinued bright line at the foramen location.

Blood flow was seen as “cine loop” videos generated by the collection of consecutive image frames where the B-mode display is overlaid with color pixels (Supplementary video 2). Color Doppler cine loops display blood velocity, with shades of red and blue colors, while the color power cine loops show the blood volume in the area of interest as a single-hue red color. The overlaid implant or palatal structures observed in the B-mode provide anatomical references for the blood velocity and volume image interpretation.

3.3 Blood volume changes at the implant site

In the midfacial scan, an increase in CV_m of 199% was observed compared to baseline at the 1-week follow-up. The CV_m increase in the mesial, distal and transverse scans were 102%, 95.6% and 163%, respectively, compared to baseline. The CV_m increase at 1 month was similar to the one observed at 1 week in all the scans. At the 6- and 12-month follow-up, CV_m was found to be lower than baseline (Figure 6). A similar trend was observed for CP_m change over time (Table 3 and Appendix).

3.4 Blood volume change at the palatal donor site

At the 1-week follow-up, the CV_m change was 146% at the 3-mm scan, while the 5-mm and 8-mm scan showed a CV_m increase of 179% and 222%, respectively compared to baseline. The CV_m increase at 1-month was found to be still higher than baseline values in all the scans. At the 6- and 12-month recalls, similar CV_m change were found in the 3-, 5- and 8-mm scans, with minimal differences compared to baseline CV_m. The CV_m at the GPF area showed an increase of 50.1% after 1 week, 40.8% after 1 month, 11.8% after 6 months and 4.81% after 12 months (Figure 7). Table 4 and Appendix depict CV_m and CP_m over the 12-month observation period at the palatal site.

4. Discussion

Power Doppler US has grown to be a full portion of diagnostics across a diversity of medical specialties, in particular for distinguishing normal from abnormal blood flow (Oglat et al., 2018, Hansen et al., 2017, Goddi et al., 2017, Pinter et al., 2018, Welsh et al., 2019). Its application in dentistry and in particular in periodontics can also prove beneficial with exploring blood flow alterations around natural teeth and dental implant in a non-ionizing, chairside and cost-efficient manner with potential implications such as detecting pathological conditions, or identifying an undetectable subclinical inflammation prior to the detection of bone loss (Chan and Kripfgans, 2020b).

Earlier studies examined the vascular morphology and blood flow in healthy, or inflamed or diseased periodontia (Kennedy, 1974, Hock, 1979, Kaplan et al., 1982, Hock and Kim, 1987). They showed that induction of inflammation resulted in the development of collateral circulation from the periodontal ligament to the gingiva (Kennedy, 1974), that could explain the increased blood flow in

the presence of gingivitis (Hock and Kim, 1987) or periodontal disease (Kaplan et al., 1982). In particular, sites with moderate to severe periodontitis demonstrated a much greater blood flow (250-400%) than sites with minimal periodontal destruction (Kaplan et al., 1982). Nevertheless, their method of using radiolabeled carbonized microspheres infused into the left cardiac ventricle (Hock and Kim, 1987, Kaplan et al., 1982) is not reproducible in human clinical studies, nor possible during standard clinical patient-care procedures. Some authors have evaluated gingival perfusion using laser Doppler flowmetry (Mavropoulos et al., 2001, Ambrosini et al., 2002, Patino-Marin et al., 2005, Retzepi et al., 2007, Kuraji et al., 2020). However, some limitations of this technology may include the presence of motion artifact noise, lack of quantitative units for perfusion, limited diagnostic values in smokers, and lack of studies validating this tool in periodontics (Firkova and Bouka, 2019). Fluorescein angiography has also been utilized for assessing capillary blood microcirculation after mucogingival and soft tissue grafting procedures (Mormann and Ciancio, 1977, Mormann et al., 1975, Burkhardt and Lang, 2005). Nevertheless, some of the drawback can be the prerequisite of intravenous injection of a contrast medium, progressive dye leakage that may lead to loss of vascular details, and possible side effects such as vertigo, nausea, vomiting or anaphylaxis (Burkhardt and Lang, 2005, Keane and Sadda, 2010).

The present study aimed at describing an US-based color and power pixel density (CPPD) technique for assessing blood flow and tissue perfusion changes at implant and palatal sites following connective tissue grafting procedures. While this method is well-validated in the medical field (Hernandez-Andrade et al., 2004a, Gao et al., 2013, Welsh et al., 2019), to the best of our knowledge, this is the first report of its application in Periodontics. Among the advantages of ultrasonography compared to other technologies previously utilized for assessing tissue perfusion in natural dentition, it has to be mentioned that power Doppler US allows for a non-ionizing, chair-side and real-time evaluation of blood flow and its variation over time. Despite the pilot nature of the current article and the limited sample size we observed a mean increase in blood volume at 1 week and 1 month compared to baseline values. Interestingly, at the 6- and 12-month follow-up we noticed a reduction in the mean blood flow. If these findings are confirmed in future studies, it will be possible to speculate that the decrease of subclinical inflammation compared to baseline could have been related to surgical interventions that modify the soft tissue peri-implant phenotype (Roccuzzo et al., 2016, Perussolo et al., 2018, Tavelli et al., 2020a) or that participating in this study with frequent follow-up visits may have had a positive impact on patients' motivation and oral hygiene levels resulting in a significantly decreased mucosal inflammation.

Two previous studies evaluated blood flow following soft tissue grafting (Demirkol et al., 2001, Tatarakis et al., 2018). Demirkol et al. used a xenon-133 clearance method for assessing blood circulation of free gingival grafts during the initial healing phase, showing that mean blood flow gradually increased at 10 and 20 days before reaching the initial value of the recipient area on the day

40 (Demirkol et al., 2001). Using laser Doppler flowmetry, Tatarakis et al. found that collagen matrix and CTG displayed a differing pattern of blood flow changes over time (Tatarakis et al., 2018). Due to the preliminary nature of this study, no efforts were made for performing direct or indirect comparisons between our findings and blood volume variation obtained with different technologies.

In addition, soft tissue wound healing around dental implants differs from the healing process observed in the natural dentition, with the peri-implant soft connective tissue that resembles a scar in composition, fiber orientation and vasculature (Sculean et al., 2014). Most of the blood supply of the peri-implant mucosae are provided by supraperiosteal plexuses that divides into several branches running towards the abutment surface, with the least number of vessels found close to the implant surface (Berglundh et al., 1994, Buser et al., 1992, Sculean et al., 2014). This difference in the vasculature may affect the pattern of blood volume changes during the healing compared to natural dentition.

A previous study by Molnar and coworkers evaluated blood flow changes following the single-incision palatal harvesting technique with Laser Speckle Contrast Imaging showing a strong correlation between reperfusion time and healing score (Molnar et al., 2019). Our study evaluated the CPPD of the palatal donor site following free gingival graft harvesting, which has slowly become a popular technique among clinicians (Tavelli et al., 2020a, Barootchi et al., 2020c, Tavelli et al., 2019b). The peak of CV_m was observed at 1 week for all the examined scans, with the 8-mm area displaying higher values of blood volume compared to the other palatal sites. This is in line with a cadaver study showing that a higher mean number of medium and large vessels are found in the deep palate (Tavelli et al., 2020b). It is important to highlight that even though the harvesting was performed in the premolar regions, the greater palatine artery at the area of the GPF showed an increase in blood volume at both 1-week and 1-month. This finding is in agreement with the observations from a recent wound healing model, showing major changes in the vascular network in the whole region following an injury, with the blood supply redirected to the wounded area (Yousefi et al., 2014). The increase in vessel diameters and the enlargement of the recruited collateral bridges mediate the enhancement of the blood flow, which is vital for the healing and surviving of the injured tissue (Yousefi et al., 2014).

Among the limitations of the present pilot study, the inclusion of a single light smoker (even though CPPD variations at the implant- and palatal donor site did not show a substantial difference compared to the other subjects) have to be noted. In addition, although the presented method has already been shown to be reliable and it has been validated in the medical field (Carson et al., 1998, Fleischer et al., 1999, Hernandez-Andrade et al., 2004a, Gao et al., 2013, Welsh et al., 2019), future studies comparing power Doppler US and other techniques, such as fluorescein angiography or laser Doppler flowmetry, for tissue perfusion evaluation at implant and palatal sites are needed. Future studies may benefit from power Doppler US for evaluating tissue perfusion during different phases of

periodontal/peri-implant healing, diagnosis of pathological conditions or subclinical inflammation. Definition of blood flow thresholds for health vs inflammatory or infective processes, based also on patient's characteristics and anatomical location, are therefore encouraged.

5. Conclusions

A novel ultrasound power Doppler method was developed to estimate tissue perfusion and CPPD variation, which correlates well with the course of normal oral wound healing events. Once validated, this technology can become an objective, non-ionizing and chairside method to study wound repair dynamics and tissue perfusion.

Conflict of interest: The authors do not have any financial interests, either directly or indirectly, in the products or information enclosed in the paper.

Data availability: The data that supports the finding of this study are available in the supplementary material of this article.

REFERENCES

Ambrosini, P., Cherene, S., Miller, N., Weissenbach, M. & Penaud, J. (2002) A laser Doppler study of gingival blood flow variations following periosteal stimulation. *J Clin Periodontol* **29,** 103-107. doi:10.1034/j.1600-051x.2002.290203.x.

Barootchi, S., Chan, H. L., Namazi, S. S., Wang, H. L. & Kripfgans, O. D. (2020a) Ultrasonographic characterization of lingual structures pertinent to oral, periodontal, and implant surgery. *Clin Oral Implants Res*. doi:10.1111/clr.13573.

Barootchi, S., Ravida, A., Tavelli, L. & Wang, H. L. (2020b) Nonsurgical treatment for peri-implant mucositis: A systematic review and meta-analysis. *Int J Oral Implantol (Berl)* **13,** 123-139.

Barootchi, S., Tavelli, L., Zucchelli, G., Giannobile, W. V. & Wang, H. L. (2020c) Gingival phenotype modification therapies on natural teeth: A network meta-analysis. *J Periodontol*. doi:10.1002/JPER.19-0715.

Berglundh, T., Lindhe, J., Jonsson, K. & Ericsson, I. (1994) The topography of the vascular systems in the periodontal and peri-implant tissues in the dog. *J Clin Periodontol* **21,** 189-193. doi:10.1111/j.1600-051x.1994.tb00302.x.

Bhaskar, V., Chan, H. L., MacEachern, M. & Kripfgans, O. D. (2018) Updates on ultrasound research in implant dentistry: a systematic review of potential clinical indications. *Dentomaxillofac Radiol* **47,** 20180076. doi:10.1259/dmfr.20180076.

Bude, R. O., Rubin, J. M. & Adler, R. S. (1994) Power versus conventional color Doppler sonography: comparison in the depiction of normal intrarenal vasculature. *Radiology* **192,** 777-780. doi:10.1148/radiology.192.3.8058946.

Burkhardt, R. & Lang, N. P. (2005) Coverage of localized gingival recessions: comparison of micro- and macrosurgical techniques. *J Clin Periodontol* **32,** 287-293. doi:10.1111/j.1600-051X.2005.00660.x.

Buser, D., Weber, H. P., Donath, K., Fiorellini, J. P., Paquette, D. W. & Williams, R. C. (1992) Soft tissue reactions to non-submerged unloaded titanium implants in beagle dogs. *J Periodontol* **63,** 225-235. doi:10.1902/jop.1992.63.3.225.

Carson, P. L., Fowlkes, J. B., Roubidoux, M. A., Moskalik, A. P., Govil, A., Normolle, D., LeCarpentier, G., Nattakom, S., Helvie, M. & Rubin, J. M. (1998) 3-D color Doppler image quantification of breast masses. *Ultrasound Med Biol* **24,** 945-952. doi:10.1016/s0301-5629(98)00055-6.

Chan, H. L. & Kripfgans, O. D. (2020a) Examination, Diagnosis and Treatment Outcome Evaluation. In: *Dental Ultrasound in Periodontology and Implantology*.

Chan, H. L. & Kripfgans, O. D. (2020b) Ultrasonography for diagnosis of peri-implant diseases and conditions: a detailed scanning protocol and case demonstration. *Dentomaxillofac Radiol***,** 20190445. doi:10.1259/dmfr.20190445.

Chan, H. L., Sinjab, K., Chung, M. P., Chiang, Y. C., Wang, H. L., Giannobile, W. V. & Kripfgans, O. D. (2017a) Non-invasive evaluation of facial crestal bone with ultrasonography. *PLoS One* **12,** e0171237. doi:10.1371/journal.pone.0171237.

Chan, H. L., Sinjab, K., Li, J., Chen, Z., Wang, H. L. & Kripfgans, O. D. (2018) Ultrasonography for noninvasive and real-time evaluation of peri-implant tissue dimensions. *J Clin Periodontol*. doi:10.1111/jcpe.12918.

Chan, H. L., Wang, H. L., Fowlkes, J. B., Giannobile, W. V. & Kripfgans, O. D. (2017b) Non-ionizing real-time ultrasonography in implant and oral surgery: A feasibility study. *Clin Oral Implants Res* **28,** 341-347. doi:10.1111/clr.12805.

Demirkol, A., Demirkol, M. O., Demirel, K., Meric, H. & Cantez, S. (2001) Blood flow of free gingival grafts measured by xenon-133 clearance. *Periodontal Clin Investig* **23,** 15-19.

Firkova, E. & Bouka, M. (2019) Laser Doppler Flowmetry in the Evaluation of Periodontal Health and Disease. *J of IMAB* **25,** 2599-2602. doi:https://doi.org/10.5272/jimab.2019253.2599.

Fleischer, A. C., Wojcicki, W. E., Donnelly, E. F., Pickens, D. R., Thirsk, G., Thurman, G. B. & Hellerqvist, C. G. (1999) Quantified color Doppler sonography of tumor vascularity in an animal model. *J Ultrasound Med* **18,** 547-551. doi:10.7863/jum.1999.18.8.547.

Fu, J. H., Hasso, D. G., Yeh, C. Y., Leong, D. J., Chan, H. L. & Wang, H. L. (2011) The accuracy of identifying the greater palatine neurovascular bundle: a cadaver study. *J Periodontol* **82,** 1000-1006. doi:10.1902/jop.2011.100619.

Gao, J., Chevalier, J., Auh, Y. H., Rubin, J. M., Wang, H., Sun, L. N., Seshan, S. & Min, R. (2013) Correlation between Doppler parameters and renal cortical fibrosis in lupus nephritis: a preliminary observation. *Ultrasound Med Biol* **39,** 275-282. doi:10.1016/j.ultrasmedbio.2012.10.009.

Goddi, A., Fanizza, M., Bortolotto, C., Raciti, M. V., Fiorina, I., He, X., Du, Y. & Calliada, F. (2017) Vector flow imaging techniques: An innovative ultrasonographic technique for the study of blood flow. *J Clin Ultrasound* **45,** 582-588. doi:10.1002/jcu.22519.

Hansen, K. L., Nielsen, M. B. & Jensen, J. A. (2017) Vector velocity estimation of blood flow - A new application in medical ultrasound. *Ultrasound* **25,** 189-199. doi:10.1177/1742271X17713353.

Hashim, D., Cionca, N., Combescure, C. & Mombelli, A. (2018) The diagnosis of peri-implantitis: A systematic review on the predictive value of bleeding on probing. *Clin Oral Implants Res* **29 Suppl 16,** 276-293. doi:10.1111/clr.13127.

Hernandez-Andrade, E., Jansson, T., Figueroa-Diesel, H., Rangel-Nava, H., Acosta-Rojas, R. & Gratacos, E. (2007) Evaluation of fetal regional cerebral blood perfusion using power

Doppler ultrasound and the estimation of fractional moving blood volume. *Ultrasound Obstet Gynecol* **29,** 556-561. doi:10.1002/uog.4005.

Hernandez-Andrade, E., Jansson, T., Ley, D., Bellander, M., Persson, M., Lingman, G. & Marsal, K. (2004a) Validation of fractional moving blood volume measurement with power Doppler ultrasound in an experimental sheep model. *Ultrasound Obstet Gynecol* **23,** 363-368. doi:10.1002/uog.1002.

Hernandez-Andrade, E., Thuring-Jonsson, A., Jansson, T., Lingman, G. & Marsal, K. (2004b) Fractional moving blood volume estimation in the fetal lung using power Doppler ultrasound: a reproducibility study. *Ultrasound Obstet Gynecol* **23,** 369-373. doi:10.1002/uog.1003.

Hock, J. (1979) Vascular morphology in noninflamed healed gingiva of dogs. *J Clin Periodontol* **6,** 37-44. doi:10.1111/j.1600-051x.1979.tb02289.x.

Hock, J. M. & Kim, S. (1987) Blood flow in healed and inflamed periodontal tissues of dogs. *J Periodontal Res* **22,** 1-5. doi:10.1111/j.1600-0765.1987.tb01532.x.

Kaplan, M. L., Jeffcoat, M. K. & Goldhaber, P. (1982) Blood flow in gingiva and alveolar bone in beagles with periodontal disease. *J Periodontal Res* **17,** 384-389. doi:10.1111/j.1600-0765.1982.tb01169.x.

Keane, P. A. & Sadda, S. R. (2010) Imaging chorioretinal vascular disease. *Eye (Lond)* **24,** 422-427. doi:10.1038/eye.2009.309.

Kennedy, J. E. (1974) Effect of inflammation on collateral circulation of the gingiva. *J Periodontal Res* **9,** 147-152. doi:10.1111/j.1600-0765.1974.tb00666.x.

Kuraji, R., Wu, Y. H., Hashimoto, S., Mishiro, S., Maeda, Y., Miyashita, Y., Ito, H., Miwa, Y., Sunohara, M., Kapila, Y. & Numabe, Y. (2020) Temporal and dynamic changes in gingival blood flow during progression of ligature-induced periodontitis. *Oral Dis*. doi:10.1111/odi.13328.

Lai, P. K., Wang, Y. A. & Welsh, A. W. (2010) Reproducibility of regional placental vascularity/perfusion measurement using 3D power Doppler. *Ultrasound Obstet Gynecol* **36,** 202-209. doi:10.1002/uog.7608.

Levy, B. I., Schiffrin, E. L., Mourad, J. J., Agostini, D., Vicaut, E., Safar, M. E. & Struijker-Boudier, H. A. (2008) Impaired tissue perfusion: a pathology common to hypertension, obesity, and diabetes mellitus. *Circulation* **118,** 968-976. doi:10.1161/CIRCULATIONAHA.107.763730.

Mavropoulos, A., Aars, H. & Brodin, P. (2001) The acute effects of smokeless tobacco (snuff) on gingival blood flow in man. *J Periodontal Res* **36,** 221-226. doi:10.1034/j.1600-0765.2001.036004221.x.

Molnar, B., Molnar, E., Fazekas, R., Ganti, B., Mikecs, B. & Vag, J. (2019) Assessment of Palatal Mucosal Wound Healing Following Connective-Tissue Harvesting by Laser Speckle Contrast Imaging: An Observational Case Series Study. *Int J Periodontics Restorative Dent* **39,** e64-e70. doi:10.11607/prd.3878.

Mormann, W., Bernimoulin, J. P. & Schmid, M. O. (1975) Fluorescein angiography of free gingival autografts. *J Clin Periodontol* **2,** 177-189. doi:10.1111/j.1600-051x.1975.tb01740.x.

Mormann, W. & Ciancio, S. G. (1977) Blood supply of human gingiva following periodontal surgery. A fluorescein angiographic study. *J Periodontol* **48,** 681-692. doi:10.1902/jop.1977.48.11.681.

Newman, J. S., Adler, R. S., Bude, R. O. & Rubin, J. M. (1994) Detection of soft-tissue hyperemia: value of power Doppler sonography. *AJR Am J Roentgenol* **163,** 385-389. doi:10.2214/ajr.163.2.8037037.

Oglat, A. A., Matjafri, M. Z., Suardi, N., Oqlat, M. A., Abdelrahman, M. A. & Oqlat, A. A. (2018) A Review of Medical Doppler Ultrasonography of Blood Flow in General and Especially in Common Carotid Artery. *J Med Ultrasound* **26,** 3-13. doi:10.4103/JMU.JMU_11_17.

Patino-Marin, N., Martinez, F., Loyola-Rodriguez, J. P., Tenorio-Govea, E., Brito-Orta, M. D. & Rodriguez-Martinez, M. (2005) A novel procedure for evaluating gingival perfusion status using laser-Doppler flowmetry. *J Clin Periodontol* **32,** 231-237. doi:10.1111/j.1600-051X.2005.00655.x.

Perussolo, J., Souza, A. B., Matarazzo, F., Oliveira, R. P. & Araujo, M. G. (2018) Influence of the keratinized mucosa on the stability of peri-implant tissues and brushing discomfort: A 4-year follow-up study. *Clin Oral Implants Res* **29,** 1177-1185. doi:10.1111/clr.13381.

Pinter, S. Z., Kripfgans, O. D., Treadwell, M. C., Kneitel, A. W., Fowlkes, J. B. & Rubin, J. M. (2018) Evaluation of Umbilical Vein Blood Volume Flow in Preeclampsia by Angle-Independent 3D Sonography. *J Ultrasound Med* **37,** 1633-1640. doi:10.1002/jum.14507.

Renvert, S., Persson, G. R., Pirih, F. Q. & Camargo, P. M. (2018) Peri-implant health, peri-implant mucositis, and peri-implantitis: Case definitions and diagnostic considerations. *J Clin Periodontol* **45 Suppl 20,** S278-S285. doi:10.1111/jcpe.12956.

Retzepi, M., Tonetti, M. & Donos, N. (2007) Comparison of gingival blood flow during healing of simplified papilla preservation and modified Widman flap surgery: a clinical trial using laser Doppler flowmetry. *J Clin Periodontol* **34,** 903-911. doi:10.1111/j.1600-051X.2007.01119.x.

Roccuzzo, M., Grasso, G. & Dalmasso, P. (2016) Keratinized mucosa around implants in partially edentulous posterior mandible: 10-year results of a prospective comparative study. *Clin Oral Implants Res* **27,** 491-496. doi:10.1111/clr.12563.

Rubin, J. M., Adler, R. S., Fowlkes, J. B., Spratt, S., Pallister, J. E., Chen, J. F. & Carson, P. L. (1995) Fractional moving blood volume: estimation with power Doppler US. *Radiology* **197,** 183-190. doi:10.1148/radiology.197.1.7568820.

Rubin, J. M., Bude, R. O., Carson, P. L., Bree, R. L. & Adler, R. S. (1994) Power Doppler US: a potentially useful alternative to mean frequency-based color Doppler US. *Radiology* **190,** 853-856. doi:10.1148/radiology.190.3.8115639.

Rubin, J. M., Bude, R. O., Fowlkes, J. B., Spratt, R. S., Carson, P. L. & Adler, R. S. (1997) Normalizing fractional moving blood volume estimates with power Doppler US: defining a stable intravascular point with the cumulative power distribution function. *Radiology* **205,** 757-765. doi:10.1148/radiology.205.3.9393532.

Sculean, A., Gruber, R. & Bosshardt, D. D. (2014) Soft tissue wound healing around teeth and dental implants. *J Clin Periodontol* **41 Suppl 15,** S6-22. doi:10.1111/jcpe.12206.

Stevenson, G. N., Collins, S. L., Welsh, A. W., Impey, L. W. & Noble, J. A. (2015) A technique for the estimation of fractional moving blood volume by using three-dimensional power Doppler US. *Radiology* **274,** 230-237. doi:10.1148/radiol.14132363.

Tatarakis, N., Gkranias, N., Darbar, U. & Donos, N. (2018) Blood flow changes using a 3D xenogeneic collagen matrix or a subepithelial connective tissue graft for root coverage procedures: a pilot study. *Clin Oral Investig* **22,** 1697-1705. doi:10.1007/s00784-017-2261-5.

Tattan, M., Sinjab, K., Lee, E., Arnett, M., Oh, T. J., Wang, H. L., Chan, H. L. & Kripfgans, O. D. (2019) Ultrasonography for chairside evaluation of periodontal structures: A pilot study. *J Periodontol*. doi:10.1002/JPER.19-0342.

Tavelli, L., Asa'ad, F., Acunzo, R., Pagni, G., Consonni, D. & Rasperini, G. (2018) Minimizing Patient Morbidity Following Palatal Gingival Harvesting: A Randomized Controlled Clinical Study. *Int J Periodontics Restorative Dent* **38,** e127-e134. doi:10.11607/prd.3581.

Tavelli, L., Barootchi, S., Avila-Ortiz, G., Urban, I. A., Giannobile, W. V. & Wang, H. L. (2020a) Peri-implant soft tissue phenotype modification and its impact on peri-implant health: A systematic review and network meta-analysis. *J Periodontol*. doi:10.1002/JPER.19-0716.

Tavelli, L., Barootchi, S., Namazi, S. S., Chan, H. L., Brzezinski, D., Danciu, T. & Wang, H. L. (2020b) The influence of palatal harvesting technique on the donor site vascular injury: A split-mouth comparative cadaver study. *J Periodontol* **91,** 83-92. doi:10.1002/JPER.19-0073.

Tavelli, L., Barootchi, S., Ravida, A., Oh, T. J. & Wang, H. L. (2019a) What Is the Safety Zone for Palatal Soft Tissue Graft Harvesting Based on the Locations of the Greater Palatine Artery and Foramen? A Systematic Review. *J Oral Maxillofac Surg* **77,** 271 e271-271 e279. doi:10.1016/j.joms.2018.10.002.

Tavelli, L., Ravida, A., Saleh, M. H. A., Maska, B., Del Amo, F. S., Rasperini, G. & Wang, H. L. (2019b) Pain perception following epithelialized gingival graft harvesting: a randomized clinical trial. *Clin Oral Investig* **23,** 459-468. doi:10.1007/s00784-018-2455-5.

Vosborg, F., Malmqvist, L. & Hamann, S. (2020) Non-invasive measurement techniques for quantitative assessment of optic nerve head blood flow. *Eur J Ophthalmol* **30,** 235-244. doi:10.1177/1120672119858891.

Welsh, A. (2004) Quantification of power Doppler and the index 'fractional moving blood volume' (FMBV). *Ultrasound Obstet Gynecol* **23,** 323-326. doi:10.1002/uog.1037.

Welsh, A. W., Fowlkes, J. B., Pinter, S. Z., Ives, K. A., Owens, G. E., Rubin, J. M., Kripfgans, O. D., Looney, P., Collins, S. L. & Stevenson, G. N. (2019) Three-dimensional US Fractional Moving Blood Volume: Validation of Renal Perfusion Quantification. *Radiology* **293,** 460-468. doi:10.1148/radiol.2019190248.

Yousefi, S., Qin, J., Dziennis, S. & Wang, R. K. (2014) Assessment of microcirculation dynamics during cutaneous wound healing phases in vivo using optical microangiography. *J Biomed Opt* **19,** 76015. doi:10.1117/1.JBO.19.7.076015.

Zucchelli, G., Mazzotti, C., Mounssif, I., Marzadori, M. & Stefanini, M. (2013) Esthetic treatment of peri-implant soft tissue defects: a case report of a modified surgical-prosthetic approach. *Int J Periodontics Restorative Dent* **33,** 327-335. doi:10.11607/prd.1632.

Zucchelli, G., Tavelli, L., Stefanini, M., Barootchi, S., Mazzotti, C., Gori, G. & Wang, H. L. (2019) Classification of facial peri-implant soft tissue dehiscence/deficiencies at single implant sites in the esthetic zone. *J Periodontol* **90,** 1116-1124. doi:10.1002/JPER.18-0616.

Tables and Figures

Table 1. Characteristics of patients at baseline and ultrasonographic analysis at the implant sites

Table 2. Baseline characteristics at the palatal donor site

Table 3. Changes in color velocity and color power over the 12-month observation period at implant sites

Table 4. Color velocity and color power variation over the 12-month observation period at the palatal site

Figure 1. Miniature-sized probe prototype (L25-8). A) Frontal view. B) Lateral view. C) Frontal view of the probe after its preparation for clinical use. D) Ultrasound gel applied on the probe. E) Clinical picture showing the application of the ultrasound probe at the midfacial aspect of an implant site (left central incisor).

Figure 2. B-mode scan of the implant site showing the ultrasonographic imaging at the mesial-, midfacial-, distal- and transverse scan. Legend. A: abutment; B: bone plate; C: crown of the implant; CB: crestal bone; I: implant; ST: soft tissue.

Figure 3. B-mode scan of the palate showing the scan obtained 3-mm, 5-mm and 8-mm from the gingival margin of the second premolar prior to the harvesting. A scan in the region of the greater palatine foramen was also performed. Legend. GPF: greater palatine foramen; PB: palatal bone. ST: Soft tissue.

Figure 4. Color velocity and color power at the midfacial, mesial and distal scans. The displayed color velocity visualizes the speed at which blood flows, while color power shows the amount of blood flowing within the lumens in the field of view. Color velocity imaging was performed using a constant velocity scale (±2.3 cm/s), with the color red indicating blood flow towards the transducer, and the blue color denotes blood flow in the opposite direction. Color power is displayed in a single-hue red color.

Figure 5. Definition of the region of interest (ROI) at the midfacial (A) and transverse (B) scans of the implant site and at the 5-mm palatal scan (C). The ROI includes the soft tissue component only, with the same anatomical references that are using to define the ROI at different time points.

Figure 6. Ultrasound color mode at the implant site at the midfacial, transverse, mesial and distal scan, showing the variation in color velocity at baseline, 1-week, 1-month, 6-month and 12-month post-op.

Figure 7. Ultrasound color mode at the palatal sites at different time points. An increase in blood volume was observed in all the scans (3 mm, 5 mm, 8 mm and greater palatal foramen [GPF]) at the 1-week and 1-month follow-up, compared to baseline.

Supplementary files

Supplementary video 1. Speed-weighted (CV_w) and power-weighted (CP_w) color pixel density computed using custom scripts for Matlab (The Mathworks, Natick, MA)

Supplementary video 2. Color velocity change over time at the implant site following soft tissue augmentation with connective tissue graft.

Table 1. Characteristics of patients at baseline and ultrasonographic analysis at the implant sites.

Variable	Baseline characteristics
Age (mean ± SD) (years)	52.2 ± 11.1
Sex (M/F)	0/5
Smokers (n)	1 (4 cigarettes/day)
Sites	1 maxillary central incisor, 1 maxillary lateral incisor and 3 mandibular premolars
PSTD class IIa	1
PSTD class IIb	4
PD (mean ± SD) (mm) **	2.7 ± 0.6
MRec (mean ± SD) (mm) *	1.97 ± 0.39
MT at 1 mm (mean ± SD) (mm) *	0.69 ± 0.26
MT at 3 mm (mean ± SD) (mm) *	1.2 ± 0.2
MT at 5 mm (mean ± SD) (mm) *	1.39 ± 0.76
CPPD Midfacial (mean ± SD) (cm/s and fractional-pixel) *	0.12 ± 0.04 (CV) / 0.54 ± 0.08 (CP)
CPPD Mesial (mean ± SD) (cm/s and fractional-pixel) *	0.15 ± 0.06 (CV) / 0.59 ± 0.09 (CP)
CPPD Distal (mean ± SD) (cm/s and fractional-pixel) *	0.16 ± 0.05 (CV) / 0.61 ± 0.09 (CP)
CPPD Transverse (mean ± SD) (cm/s and fractional-pixel) *	0.13 ± 0.04 (CV) / 0.58 ± 0.08 (CP)

Legend. PSTD: peri-implant soft tissue dehiscence/deficiency. PD: probing depth. MRec: Mucosal recession depth. MT: mucosal thickness. CPPD: color and power pixel density. CV: color velocity. CP: color power. n: number. M: male. F: Female. mm: millimeter. cm: centimeter. SD: standard deviation.

* measured with ultrasound

** measured using a periodontal probe (PCP UNC 15, Hu-Friedy, Chicago, USA).

Table 2. Baseline characteristics and blood volume at the palatal donor site.

Variable	3-mm scan	5-mm scan	8-mm scan	GPF scan
Palatal thickness (mean ± SD) (mm)	3.49 ± 0.36	4.13 ± 0.67	4.48 ± 0.67	5.98 ± 0.84
CV (mean ± SD) (cm/s)	0.14 ± 0.05	0.17 ± 0.07	0.18 ± 0.1	0.18 ± 0.09
CP (mean ± SD) (fractional-pixel)	0.62 ± 0.08	0.62 ± 0.11	0.61 ± 0.08	0.64 ± 0.11

Legend. CV: color velocity. CP: color power. GPF: greater palatine foramen. mm: millimeter. cm: centimeter. s: second. SD: standard deviation.

Table 3. Changes in Color velocity and Color power over the 12-month observation period at implant sites

Time intervals	Color Velocity Change (mean ± SD) (%)				Color Power Change (mean ± SD) (%)			
	Midfacial scan	**Mesial scan**	**Distal scan**	**Transverse scan**	**Midfacial scan**	**Mesial scan**	**Distal scan**	**Transverse scan**
T_1-T_0	199 ± 45.6	102 ± 49.8	95.6 ± 40.9	163 ± 75.8	48.6 ± 27.1	21.8 ± 2.8	17.4 ± 7.13	32.2 ± 5.55
T_2-T_0	153 ± 44.3	97.9 ± 57.4	95.8 ± 54.3	146.9 ± 76.8	58.89 ± 38.6	33.5 ± 14.9	20.4 ± 5.14	56.1 ± 8.14
T_3-T_0	-31.5 ± 13.5	-11.8 ± 5.34	-23.6 ± 6.63	-17.5 ± 9.23	-9.27 ± 11.2	-8.54 ± 5.29	-14.2 ± 8.49	-4.48 ± 11.5
T_4-T_0	-34.2 ± 29.7	-8.93 ± 23.1	-5.48 ± 8.87	-2.47 ± 28.9	-12.5 ± 6.25	-10.9 ± 10.4	-12.1 ± 10.6	-6.80 ± 7.31

Legend. T_0: baseline. T_1: 1-week post-op. T_2: 1-month post-op. T_3:6-month post-op. T_4: 12-month post-op. CV: color velocity. CP: color power. SD: standard deviation. The changes were computed by subtracting the color velocity or color power at a follow-up time point to the respective value at baseline. Negative color velocity or color power changes indicate a reduction in the blood volume at the follow-up compared to baseline.

Table 4. Color velocity and color power variation over the 12-month observation period at the palatal site

Time intervals	Color Velocity Change (mean ± SD) (%)				Color Power Change (mean ± SD) (%)			
	3 mm scan	**5 mm scan**	**8 mm scan**	**GPF scan**	**3 mm scan**	**5 mm scan**	**8 mm scan**	**GPF scan**
T_1-T_0	146 ± 62.7	179 ± 84.7	222 ± 40.9	50.1 ± 22.4	39.9 ± 10.6	39.3 ± 19.7	44.5 ± 15.7	19.8 ± 3.50
T_2-T_0	185 ± 68.7	127 ± 59.6	178 ± 83.1	40.8 ± 22.5	37.2 ± 24.2	39.4 ± 26.8	28.8 ± 14.4	20.9 ± 10.7
T_3-T_0	5.84 ± 6.19	9.11 ± 7.29	7.84 ± 7.18	11.8 ± 9.36	3.91 ± 5.84	1.78 ± 6.75	4.92 ± 1.79	4.16 ± 6.43
T_4-T_0	4.58 ± 14.7	4.64 ± 15.9	2.53 ± 9.05	4.81 ± 9.98	0.790 ± 5.16	-1.69 ± 4.34	7.51 ± 6.95	1.31 ± 9.83

Legend

d. T_0: baseline. T_1: 1-week post-op. T_2: 1-month post-op. T_3:6-month post-op. T_4: 12-month post-op. CV: color velocity. CP: color power. SD: standard deviation. The changes were computed by subtracting the color velocity or color power at follow-up to the respective value at baseline and calculating the percentage of this difference compared to the baseline value. Negative color velocity or color power changes indicate a reduction in the blood volume at the follow-up compared to baseline.

jcpe_13424_f1.tif

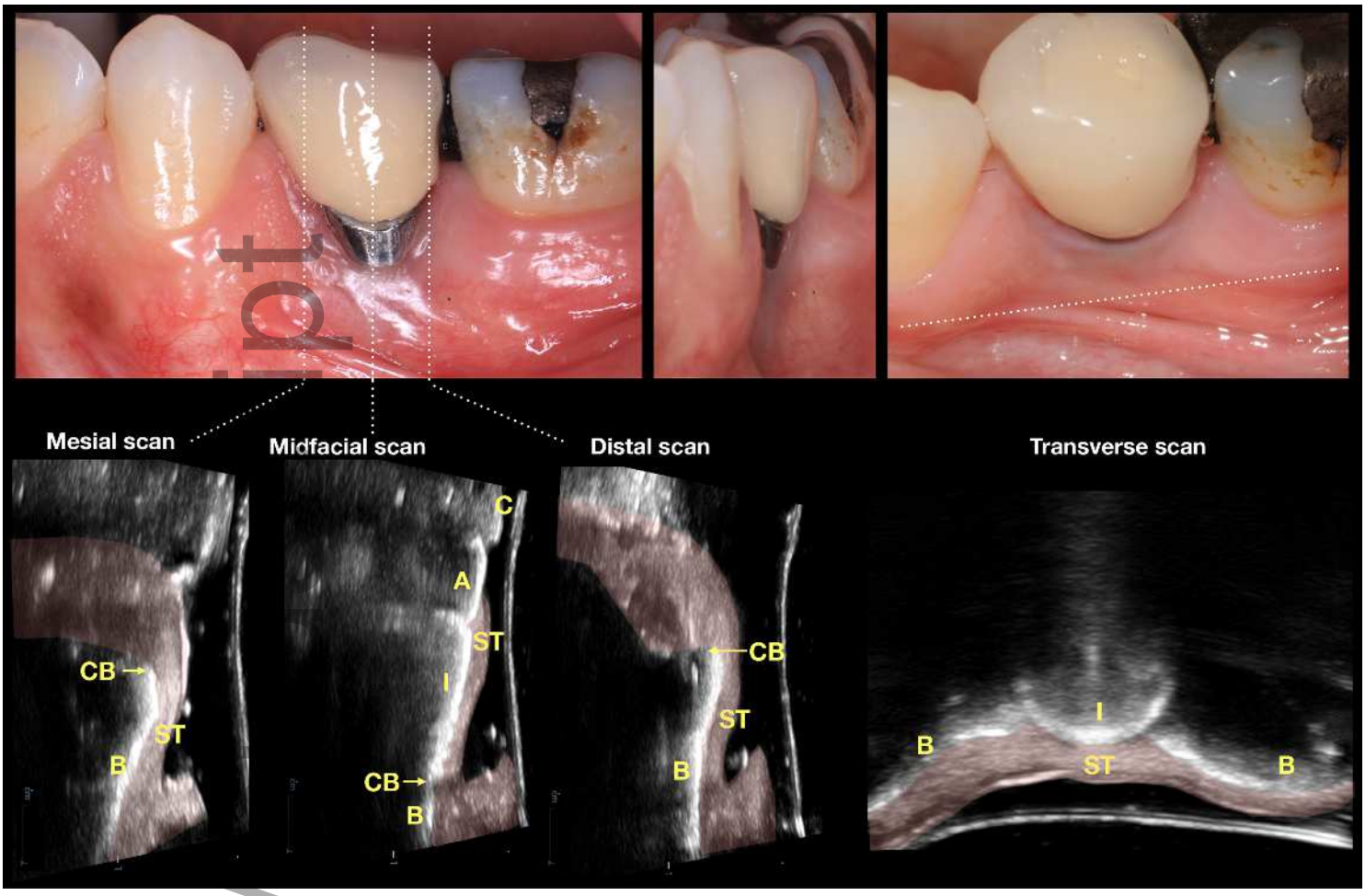

jcpe_13424_f2.tif

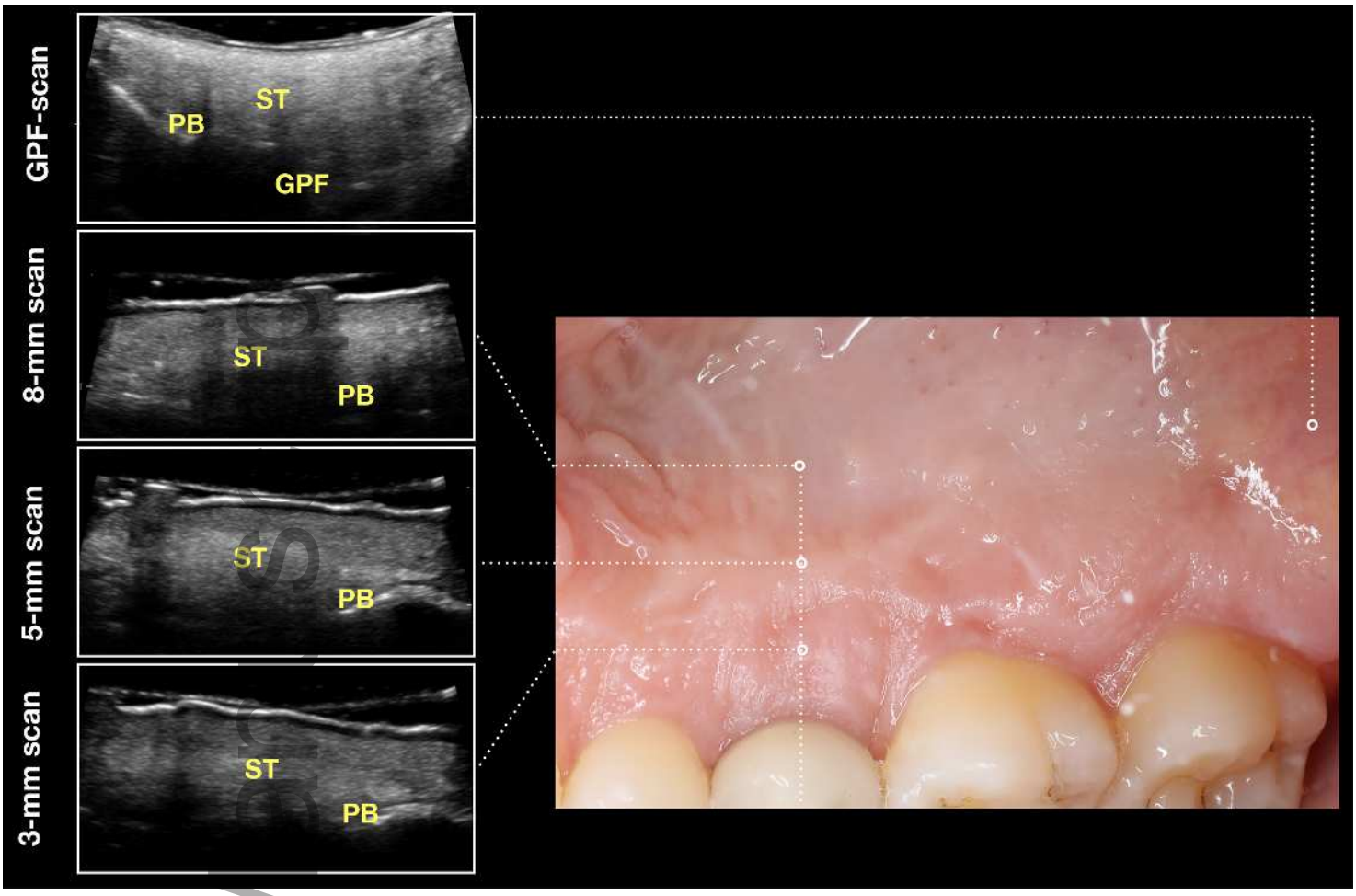

jcpe_13424_f3.tif

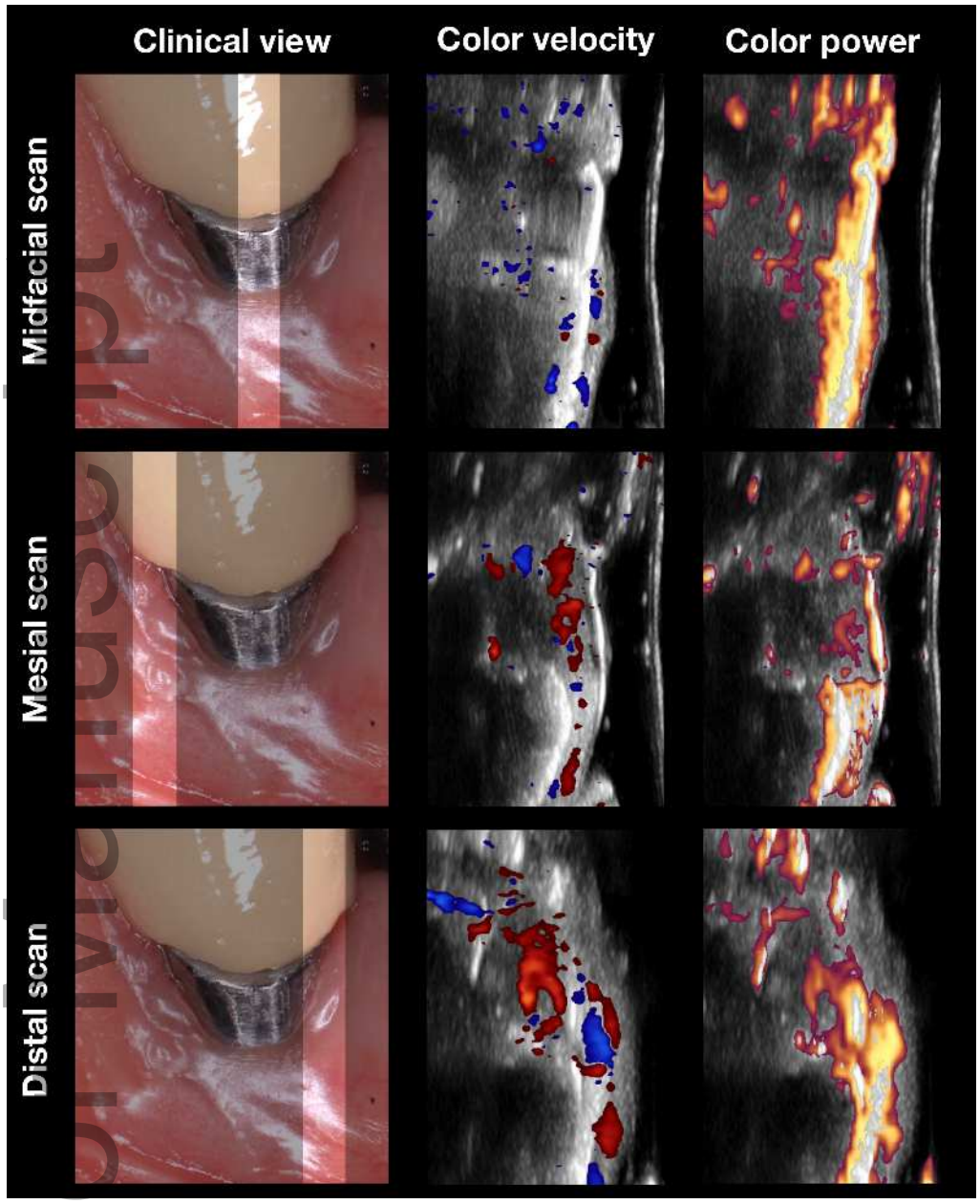

jcpe_13424_f4.tif

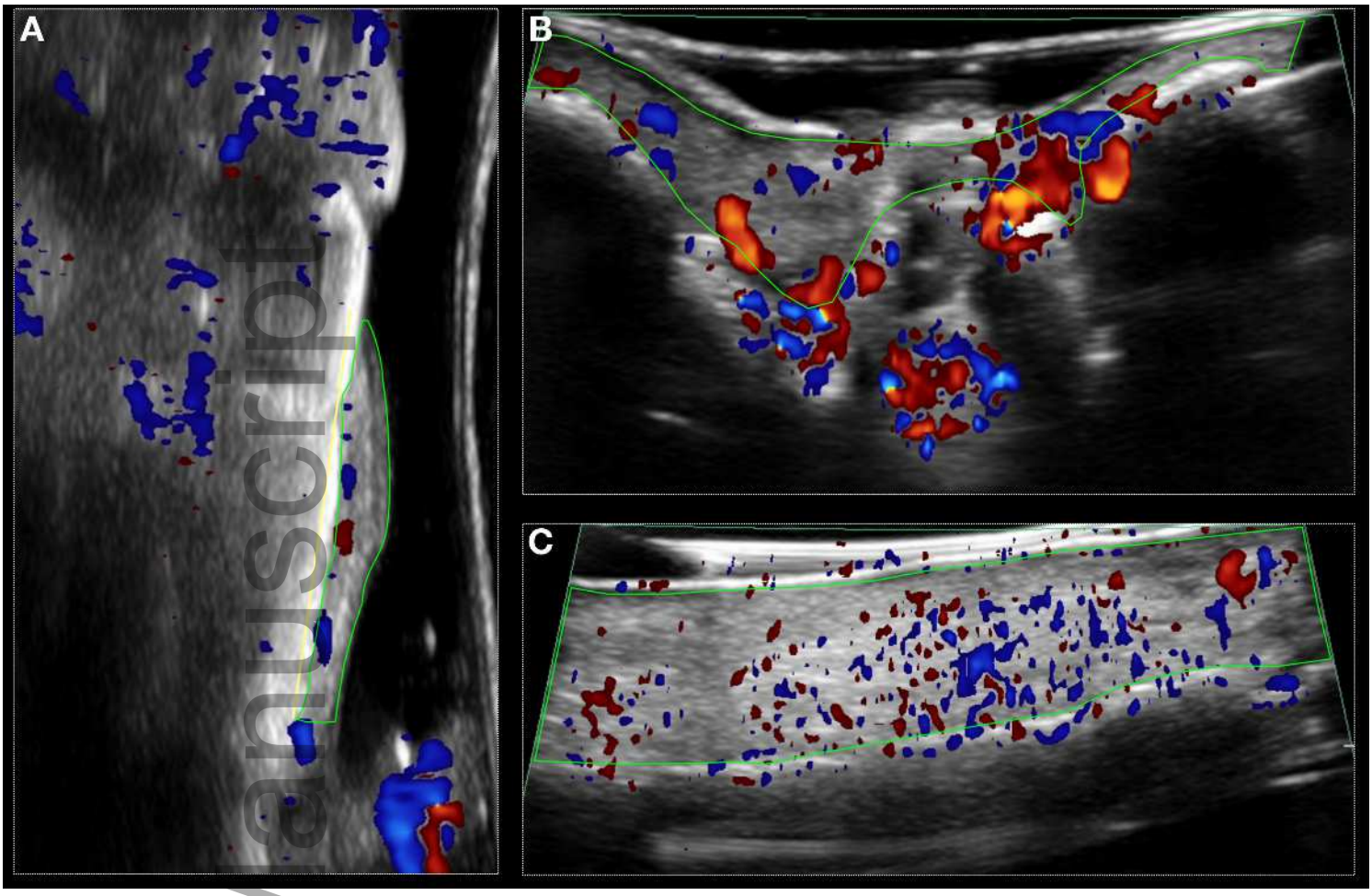

jcpe_13424_f5.tif

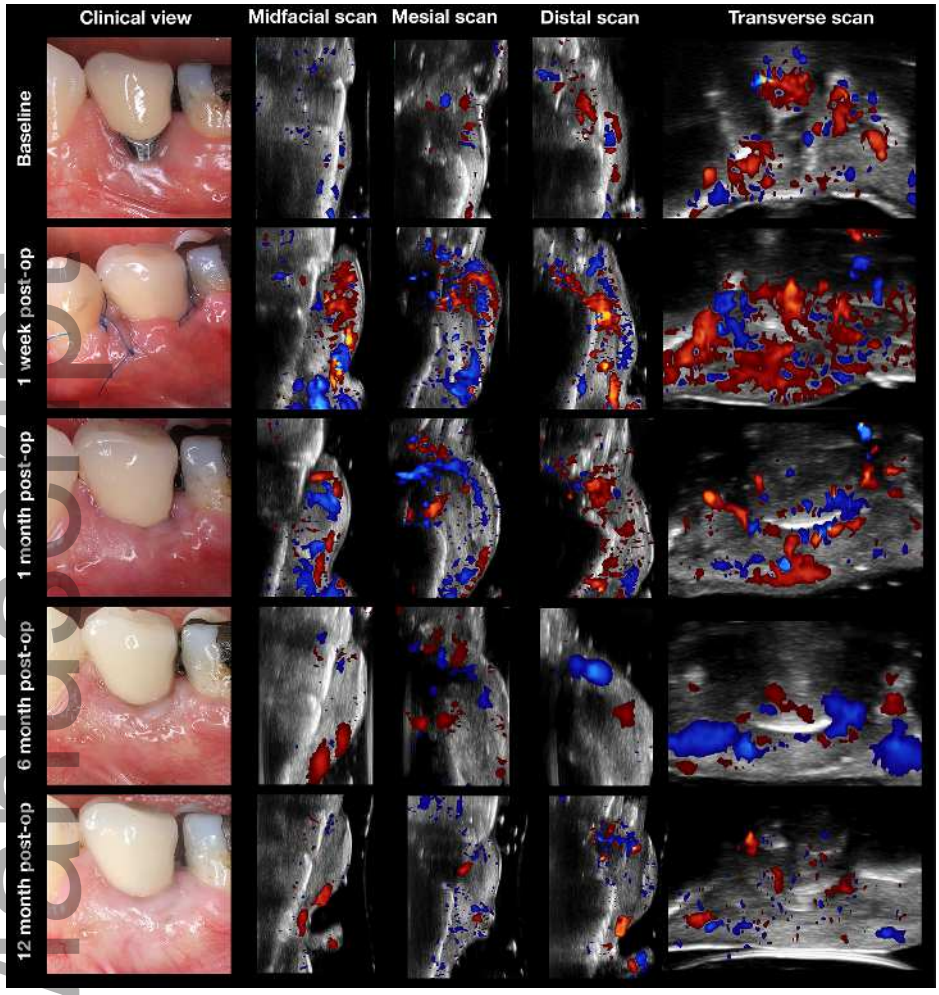

jcpe_13424_f6.tif

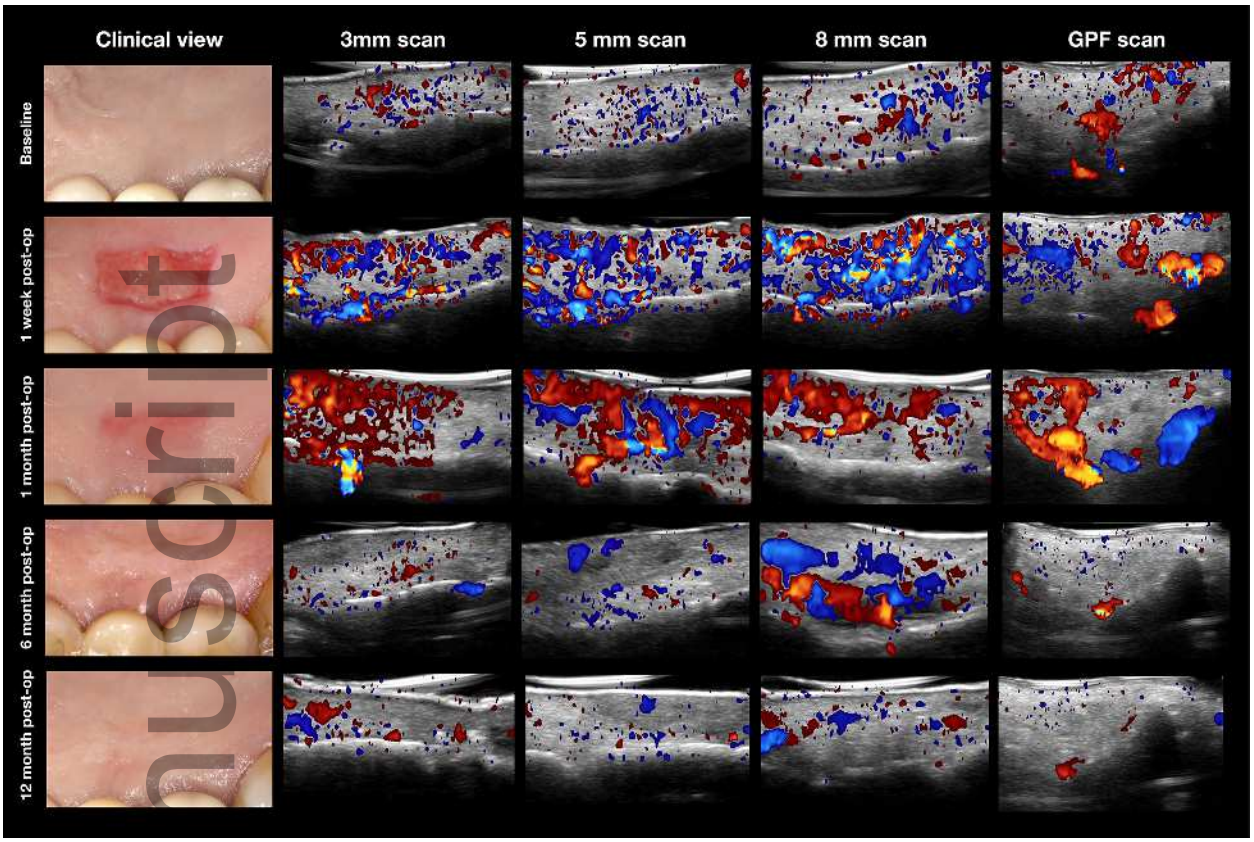

jcpe_13424_f7.tif